


RESEARCH ARTICLE

Functional connectivity of the frontotemporal network in preattentive detection of abstract changes: Perturbs and observes with transcranial magnetic stimulation and event-related optical signal

Xue-Zhen Xiao¹ | Yu-Hei Shum¹ | Troby K.-Y. Lui¹ | Yang Wang¹ |
Alexandra T.-C. Cheung¹ | Winnie C. W. Chu² | Sebastiaan F. W. Neggers³ |
Sandra S.-M. Chan⁴ | Chun-Yu Tse¹ 

¹Department of Psychology and Center for Cognition and Brain Studies, The Chinese University of Hong Kong, Hong Kong SAR, China

²Department of Imaging and Interventional Radiology, The Chinese University of Hong Kong, Hong Kong SAR, China

³Department of Psychiatry, Brain Center Rudolf Magnus, University Medical Center Utrecht, Utrecht, The Netherlands

⁴Department of Psychiatry, The Chinese University of Hong Kong, Hong Kong SAR, China

Correspondence

Chun-Yu Tse, Department of Psychology, Center for Cognition and Brain Studies, The Chinese University of Hong Kong, 328 Sino Building, CUHK, Shatin, N.T., Hong Kong SAR, China.
Email: chunytse@gmail.com

Funding information

General Research Fund, Grant/Award Number: 14606417

Abstract

Current theories of automatic or preattentive change detection suggest a regularity or prediction violation mechanism involving functional connectivity between the inferior frontal cortex (IFC) and the superior temporal cortex (STC). By disrupting the IFC function with transcranial magnetic stimulation (TMS) and recording the later STC mismatch response with event-related optical signal (EROS), previous study demonstrated a causal IFC-to-STC functional connection in detecting a pitch or physical change. However, physical change detection can be achieved by memory comparison of the physical features and may not necessarily involve regularity/rule extraction and prediction. The current study investigated the IFC–STC functional connectivity in detecting rule violation (i.e., an abstract change). Frequent standard tone pairs with a constant relative pitch difference, but varying pitches, were presented to establish a pitch interval rule. This abstract rule was violated by deviants with reduced relative pitch intervals. The EROS STC mismatch response to the deviants was abolished by the TMS applied at the IFC 80 ms after deviance onset, but preserved in the spatial (TMS on vertex), auditory (TMS sound), and temporal (200 ms after deviance onset) control conditions. These results demonstrate the IFC–STC connection in preattentive abstract change detection and support the regularity or prediction violation account.

KEYWORDS

change detection, EROS, frontotemporal network, functional connectivity, MMN, TMS

1 | INTRODUCTION

The human brain is able to detect environmental changes automatically, which is also known as preattentive change detection. Not only simple physical changes but also changes that violate invariant

relationships between events in the environment can be detected (Paavilainen, 2013; Winkler, 2007; Xiao et al., 2018). Current theories (Friston, 2005, 2010, 2011; Winkler, 2007) suggest a mechanism that involves extracting the regularity or rule from the environment for making prediction of future events. For example, when fully engaged

This is an open access article under the terms of the Creative Commons Attribution-NonCommercial-NoDerivs License, which permits use and distribution in any medium, provided the original work is properly cited, the use is non-commercial and no modifications or adaptations are made.

© 2020 The Authors. *Human Brain Mapping* published by Wiley Periodicals, Inc.

in reading a newspaper with music playing in the background, the brain is constantly monitoring the acoustic environment for unexpected events. The sound of a fire alarm is automatically detected and captures attention. An event-related brain potential (ERP) component, the mismatch negativity (MMN; Näätänen, Paavilainen, Rinne, & Alho, 2007; Näätänen & Michie, 1979), is elicited by the unexpected change. The MMN response is regarded as an error signal indicating the violation of the regularity or prediction (Friston, 2005, 2010, 2011; Winkler, 2007). MMN is typically elicited in the laboratory setting using a passive oddball paradigm, in which randomly occurring deviant events among a sequence of standard events are presented to participants who engage in an irrelevant task, such as watching a silent movie.

Earlier studies demonstrated MMNs to physical feature changes of auditory events, such as pitch (e.g., Sams, Paavilainen, Alho, & Näätänen, 1985) and intensity (e.g., Näätänen, Paavilainen, Alho, Reinikainen, & Sams, 1989). However, the detection of physical change could be achieved by comparing the physical features between the standard and deviant (Näätänen & Winkler, 1999). In other words, the regularities or rules governing the properties of the events may not be extracted and a prediction process is not necessary for detecting a physical change. The regularity or prediction violation account of preattentive change detection was supported by MMN responses to deviants violating an abstract regularity or pattern established by a train of standard events (Paavilainen, 2013; Winkler, 2007). For example, using auditory events composed of tone pairs (e.g., Sarrinen, Paavilainen, Schröger, Tervaniemi, & Näätänen, 1992), MMN was elicited by presenting deviants with rising pitch (i.e., the pitch of the second tone is relatively higher than the first tone) among standards with falling pitch (i.e., the pitch of the second tone is relatively lower than the first tone). While the absolute pitches of the tones (i.e., a physical feature) varied among the events, the regularity of the standard events could only be established by the relative pitch difference between the first and second tone (i.e., an abstract feature), but not by the absolute pitches of the tones. The regularity or prediction violation account of preattentive change detection was further demonstrated by MMNs to the violation of an abstract regularity pattern established not only by a constant abstract relationship between physical features, but also by a constant abstract relationship between abstract features, among the standard events (Xiao et al., 2018).

Under the predictive model framework of preattentive change detection (Friston, 2005, 2010; Garrido, Kilner, Kiebel, & Friston, 2007; Kiebel, Garrido, Moran, Chen, & Friston, 2009), the inferior frontal cortex (IFC) and the superior temporal cortex (STC) are hierarchically organized to establish a model for predicting future events. The model is updated to minimize the discrepancy between the predicted and the actual events. The discrepancy is regarded as the prediction error and elicits the mismatch brain responses (Winkler, 2007). The IFC is responsible for establishing or reinstating the predictive model and conveying predictive information to the STC for detecting events violating the prediction.

MMN associated mismatch responses in the IFC and the STC to physical changes have been consistently reported by using different

neuroimaging techniques, including functional magnetic resonance imaging (fMRI; Doeller et al., 2003; Molholm, Martinez, Ritter, Javitt, & Foxe, 2005; Opitz, Rinne, Mecklinger, von Cramon, & Schröger, 2002; Rinne, Degerman, & Alho, 2005; Schall, Johnston, Todd, Ward, & Michie, 2003), magnetoencephalography (Hsu, Lin, Hsu, & Lee, 2014; Lappe, Steinsträter, & Pantev, 2013; Rinne, Alho, Ilmoniemi, Virtanen, & Näätänen, 2000), electroencephalography (EEG) with source localization analysis (Caclin et al., 2006; MacLean, Blundon, & Ward, 2015; Paavilainen, Valppu, & Näätänen, 2001; Takegata, Huotilainen, Rinne, Näätänen, & Winkler, 2001; Wolff & Schröger, 2001), electrocorticography (Dürschmid et al., 2016; Phillips et al., 2016), and event-related optical signal (EROS; Rinne et al., 1999; Sable et al., 2007; Tse & Penney, 2007, 2008; Tse, Rinne, Ng, & Penney, 2013; Tse, Tien, & Penney, 2006).

By using EROS, sequential activation of the IFC and the STC in preattentive detection of physical changes, including time of occurrence and omission (Sable et al., 2007; Tse et al., 2006; Tse & Penney, 2007), frequency (Tse & Penney, 2008), duration (Rinne et al., 1999; Tse et al., 2013), and audiovisual speech sound (Tse, Gratton, Garnsey, Novak, & Fabiani, 2015), has been revealed. The right IFC response to ambiguous deviants typically began approximately 80 ms after stimulus onset and bilateral STC responses began after 120–200 ms (Tse et al., 2013; Tse & Penney, 2008). EROS measures the change in the optical property of neurons associated with a cognitive function and is able to localize brain response spatially and temporally in the subcentimeters and milliseconds scales (Gratton & Fabiani, 2001). EROS is different from another optical brain imaging method, the functional near-infrared (NIR) spectroscopy, which measures the hemodynamic response, similar to the fMRI blood oxygen level dependent (BOLD) signal. The EROS mismatch responses in the IFC and the STC correlate with simultaneously recorded ERP MMN responses (Tse et al., 2013; Tse & Penney, 2008). Thus, these EROS mismatch responses are conceptualized as the optical counterpart of the ERP MMN. However, observing an activation sequence or coactivation pattern of the IFC and the STC is not sufficient to support a causal relationship or functional connection between the two brain regions due to the correlational nature in brain imaging. For example, the observed activation sequence could be produced by a third brain region driving both mismatch responses in the IFC and the STC, but with different time delays.

Our previous study (Tse et al., 2018) evaluated the functional connectivity of the IFC and the STC in the preattentive detection of physical change by combining transcranial magnetic stimulation (TMS) with EROS (Parks, 2013). Specifically, TMS is applied to disrupt the functioning of the IFC to examine whether the IFC is critical for the later mismatch response in STC. Because the optical signal measured in EROS is inert to the electromagnetic energy of TMS, the causal connection of brain regions in generating the mismatch brain response can be examined by the combined TMS-EROS method. The critical functional role of the IFC to the later STC mismatch response was demonstrated by the abolishment of the STC response from 150 to 200 ms, when TMS was applied to the IFC 80 ms after the onset of a pitch deviant. However, the STC mismatch response remained intact when a sham TMS was applied on vertex, or when TMS was applied

to the IFC 200 ms after the onset of the deviant. This study demonstrated a functional connection between the IFC and the STC in preattentive detection of physical changes; however, it remains unknown if a similar connection between the IFC and the STC is essential for detecting abstract changes or rule violation as suggested by the regularity or prediction violation account. In fact, the IFC and STC mismatch brain responses in the brain imaging studies mentioned above were elicited by deviance in physical features. Only a few EEG studies with a distributed source localization analysis suggested the involvement of both the IFC and the STC in the preattentive detection of abstract changes, including change in the pitch pattern of a tone train (Korzyukov, Winkler, Gumenyuk, & Alho, 2003; Schröger, Bendixen, Trujillo-Barreto, & Roeber, 2007), the pitch-duration association (Bendixen, Prinz, Horváth, Trujillo-Barreto, & Schröger, 2008), as well as, the rhythmic and melodic patterns of auditory events (Lappe et al., 2013).

The current study examined whether the functioning of the IFC in the predetection stage is critical for the later STC mismatch response in detecting the violation of a pitch interval rule, by using TMS and EROS. For an auditory event consisted of a tone pair, the relative pitch interval or difference of the two tones represented an abstract property of the auditory events. The pitch differences were kept identical among the standard events to establish a pitch interval rule, while the absolute pitches of tones varied between events. The pitch interval rule was violated by deviant events with reduced pitch intervals. Larger deviance from the expected or standard pitch interval would elicit a stronger MMN response (Xiao et al., 2018). Although the EROS STC mismatch response to abstract changes has not been investigated, larger deviance in the physical feature had been consistently shown to elicit a stronger EROS STC mismatch response previously (e.g., Tse et al., 2013; Tse & Penney, 2008).

Similar to the design in our previous TMS-EROS study (Tse et al., 2018), the STC mismatch responses elicited by deviants violating the pitch interval rule were compared when TMS was applied on the IFC, on the vertex for a sham stimulation, or when only the TMS sound recording was presented. To establish the temporal specificity of the TMS effect, the STC mismatch responses were compared when TMS or TMS pulse noise was presented at the predetection stage of 80 ms or the postdetection stage of 200 ms. If the IFC plays a critical role in eliciting the later STC mismatch response to an abstract change, TMS applied on the IFC with an 80 ms delay from the deviance onset should abolish the later STC mismatch response to the abstract change. The STC mismatch responses should be intact when TMS was applied on the IFC with 200 ms delay from deviance onset, when sham TMS was applied on vertex with 80 or 200 ms delay, or when TMS sound recording was presented with 80 or 200 ms delay.

2 | METHODS

2.1 | Participants

Twenty-four university students (14 females; age 18–28 years, mean age 21.3 years) participated after giving informed consent. The study

was approved by The Joint Chinese University of Hong Kong, New Territories East Cluster Clinical Research Ethics Committee. All participants reported having normal hearing, normal or corrected-to-normal vision, no history of neurological disorders or head trauma, and no contraindication to TMS (Rossi et al., 2009; Wassermann & Wassermann, 1998). All participants were right handed according to their Edinburgh Handedness Inventory (Oldfield, 1971) scores. Each participant took part in two identical TMS-EROS sessions. The two sessions were 10–20 days apart to prevent the establishment of long-term TMS effect (Nyffeler, Hartmann, Hess, & Müri, 2008). In both sessions, the participants watched self-selected silent movies with subtitles and were told to ignore any auditory events.

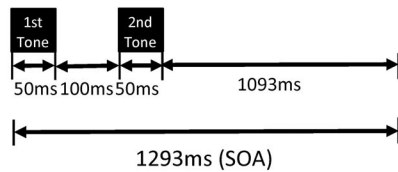
After the experiment, the participants provided responses to four questions about their conscious experience of the auditory events: (a) Did you enjoy the movie? (b) Did you pay attention to the tones presented in the background? (c) Did you notice any rule or regularity in the tone sequence? (d) Did you find any tones special or different from the others? If yes, what is the difference? All participants reported that they enjoyed the movie and did not pay attention to the tones. Twenty participants (83.33%) reported hearing the falling and rising contours of the tone pairs; however, none of them reported the rule or regularity in the tone pairs. Only two participants reported hearing tones that were different from the others, but they could not tell how these tones were different from the others. These results indicated that they were not attending to the auditory events presented.

2.2 | Stimuli and experimental design

Each auditory event presented in this study was composed of two pure tones (i.e., a tone pair). The tone frequency could be one of the 26 semitones ranging from the musical notes D4 to D6#, or from 293.66 to 1,244 Hz. In this frequency range, the perceived loudness varies minimally (Suzuki & Takeshima, 2004). The frequency difference or the number of semitone steps between the tones of a pair defined the frequency interval. An increase in frequency interval (i.e., the frequency of the second tone is higher than that of the first tone) was described as a rising contour, while a decrease in frequency interval was described as a falling contour. Each tone was 50 ms in duration which included a 5-ms rise and a 5-ms fall period. The tones of an auditory event were separated by a 100-ms silent period. The total duration of an event was 200 ms. The interevent interval was 1,093 ms (Figure 1a). The interevent interval is equivalent to the inter-trial interval as each trial was consisted of one auditory event. Previous studies (Bidelman & Chung, 2015; Denham, Gyimesi, Stefanics, & Winkler, 2013; Mittag, Takegata, & Winkler, 2016; Sable et al., 2007; Sable, Gratton, & Fabiani, 2003; Sussman, Gomes, Nousak, Ritter, & Vaughan, 1998; Xiao et al., 2018) demonstrated perceptual grouping of tones with similar spectral and temporal properties.

Similar to our previous TMS-EROS study (Tse et al., 2018), the auditory events were presented in four types of block: IFC TMS, vertex TMS control, auditory control, and equal probability control

(a) The Tone Pair of an Auditory Event



(b) Examples of Standards

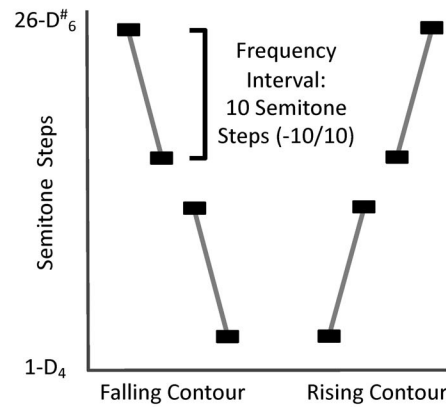
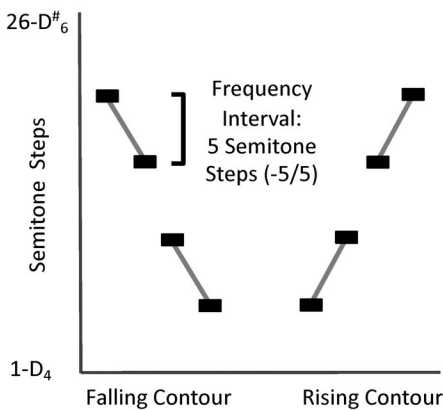
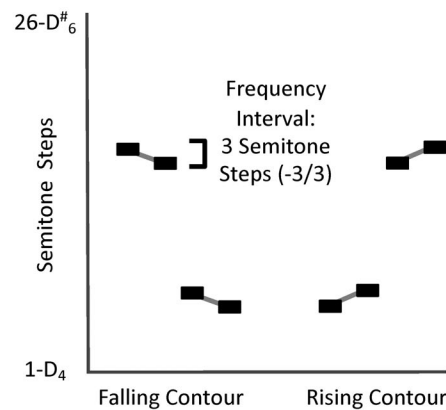


FIGURE 1 (a) The temporal structure of an auditory event, (b) examples of standards with a rising or falling contour, and examples of the (c) small and (d) large deviant events

(c) Examples of Small Deviants



(d) Examples of Large Deviants



blocks. The IFC TMS, the vertex TMS control, and the auditory control blocks shared the same auditory passive oddball design. In each of these blocks, 81.82% of the auditory events were standards while the remaining 18.28% were deviants. Half of the standards or deviants had a rising contour, while the other half had a falling contour. The stimuli with rising or falling contour were randomly presented. The mixture of the rising or falling contour could further ensure the abstract nature of the pitch interval rule. Both the standard and deviant events varied in their tone frequencies. The frequency intervals of the standards were maintained at 10 semitone steps (denoted as $-10/10$ in Figure 1b), while the frequency intervals of the deviants were either 5 semitone steps (small deviant; denoted as $-5/5$ in Figure 1c) or 3 semitone steps (large deviant; denoted as $-3/3$ in Figure 1d). Half of the deviants (9.1% of all events) was small deviants, whereas the other half was large deviants. A smaller frequency interval between the tones of an event would produce a stronger sensory adaptation effect (May & Tiitinen, 2010). With this design, a larger mismatch response elicited by the large deviant could not be explained by the release of sensory adaptation effect.

The deviant events were presented in a pseudorandom order, with the constraint that deviants were preceded by 2–7 standards. Our previous study (Tse et al., 2018) on pitch deviants showed

modulation of mismatch responses by standard train length. Mismatch responses were elicited by pitch deviants preceded by at least 4–5 standards. As the current study involved detection of abstract changes, mismatch responses were expected to be elicited by deviants preceded by a longer standard train. Consistent with this prediction, the STC mismatch responses to deviants preceded by 4–5 standards was absent in all of the control blocks. The following analyses focus on the mismatch responses to deviants preceded by 6–7 standards.

In each TMS-EROS session, each block type was repeated five times. The whole study consisted of two identical TMS-EROS sessions, and a total of 2,640 trials (2,160 standards and 480 deviants) were presented for each of the four block types. All four block types were presented in each TMS-EROS session to prevent possible confounds due to session differences. Blocks of the same type were presented in succession to shorten the time required to reposition the TMS coil. The presentation order of block types was counterbalanced across participants using the Latin square method to control for order and carryover effects among the block types. There were four presentation sequences: [A B D C], [B C A D], [C D B A], and [D A C B]; each letter represents a block type. Each presentation sequence was repeated six times and randomly assigned to the 24 participants. The

auditory events were presented using MATLAB software (MathWorks, Inc., Natick, MA) and Psychophysics Toolbox (Brainard, 1997) through a pair of Etymotic Research 2 (ER2) in-ear-type earphones (Etymotic Research, Elk Grove Village, IL).

The deviant events were paired with the application of a real TMS pulse (Figure 2). To ensure a similar auditory environment, other than the change in the frequency intervals, for the standard and deviant events, each of the standard and deviant events was also paired with a TMS sound recording. As repeated, frequent, and irregular firing of the TMS coil produces overheating, it was not possible to pair the standard events with TMS sounds produced by firing of the TMS coil. The TMS sound recording was presented by a set of speakers positioned near the TMS coil. The volume of the TMS sound recording was adjusted to mask the sound of the TMS pulse, such that the events with the TMS sound recording could not be distinguished from the events with both TMS pulse and sound recording.

Half of the standard (deviant) events was randomly paired with a TMS sound recording (with a TMS sound recording and a TMS pulse) at 80 ms after the second tone onset. For the other half, the pairing of the events and a sound recording with/without a TMS pulse took place at 200 ms after the second tone onset (Figure 2). The 80 ms delay corresponds to the latency of the IFC optical mismatch response at a predetection stage, whereas the 200 ms delay refers to a post-detection stage after the STC optical mismatch response (Tse et al., 2006, 2013; Tse & Penney, 2008). The 200 ms delay condition served as a within-block control to demonstrate that the TMS effect with 80 ms delay is specific to the predetection stage. Half of the deviant events paired with 80 or 200 ms TMS sound/pulse delay was preceded by four or five standards and the other half was preceded by six or seven standards. There were 40 deviant trials for each combination of deviance level (small/large), TMS pulse delay (80/200 ms), and standard train length (4 or 5/6 or 7).

Depending on the block type, real TMS, sham TMS, and TMS pulse noise were paired with the deviant event (Figure 3a). In the IFC TMS block, the deviant stimuli were paired with the TMS pulses applied at the right IFC. In the vertex TMS control block, the TMS was

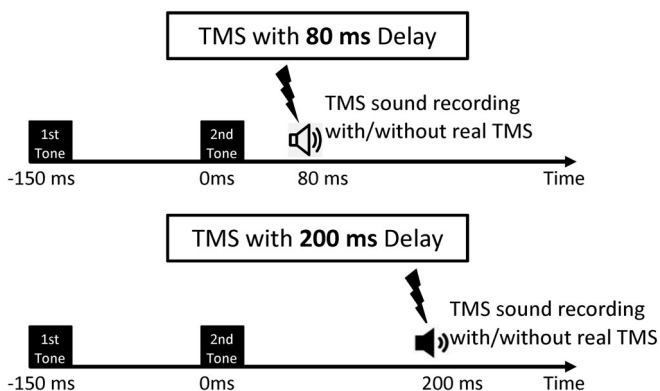


FIGURE 2 Illustration of the auditory events (tone pairs) paired with a TMS sound recording with/without a real TMS pulse at 80 ms (upper) or 200 ms (lower) after the onset of second tone. IFC, inferior frontal cortex; TMS, transcranial magnetic stimulation

applied on the vertex to control for nonlocation-specific TMS effects. Specifically, if the STC response is abolished in the IFC TMS block but preserved in the vertex TMS control block, the abolishment of the STC response in the IFC TMS block can be ascribed to the specific TMS effect at the IFC. In the auditory control block, the TMS coil was positioned next to the right IFC and rotated toward the front to deliver a TMS pulse to the empty space next to the participant's head. The auditory control block was used to measure a baseline optical mismatch response in an auditory environment similar to that of the IFC TMS and vertex TMS blocks but without TMS applied on the brain.

In the equal probability control block, the location and orientation of the TMS coil were identical to the auditory control block. Different from the oddball design of the auditory control block, 11 types of frequency intervals were presented randomly with the same probability (i.e., 9.1% for each interval; 240 trials for each interval, and 2,640 trials in total). This probability was identical to the two deviants' probabilities in the other three types of blocks. In addition to the three frequency intervals of the standard and the two deviants ($-3/3$, $-5/5$,

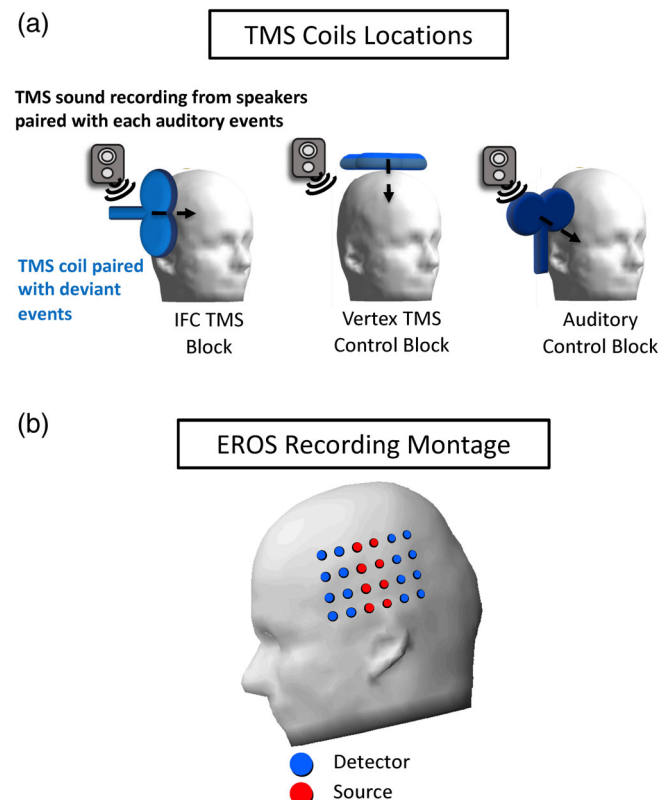


FIGURE 3 (a) The placement of TMS coils for the IFC TMS, vertex TMS control, and auditory control blocks. The blue-colored coils indicate the locations and orientations of the coils paired with the deviant event. The speakers indicate the TMS sound recordings paired with the standard, deviant, control, and filler events. (b) Montage for EROS recordings. The blue and red dots on the head model represent the locations of the 16 detector and 8 source optical fibers. EROS, event-related optical signal; IFC, inferior frontal cortex; TMS, transcranial magnetic stimulation

and $-10/10$), eight filler events with intervals, $-1/1$, $-2/2$, $-4/4$, $-6/6$, $-7/7$, $-8/8$, $-9/9$, and $-11/11$, were presented in the equal probability control block. The semitone step distributions of the first and second tones in the equal probability control block were matched with that of the other three block types. By subtracting the EROS responses of the physically identical control events presented with the matched semitone step distributions in the equal probability control block from EROS responses of the deviants presented in other three types of block, the genuine EROS mismatch responses could be obtained (Jacobsen & Schröger, 2001).

The paradigm design and comparison procedure ensure that the mismatch brain responses could not be elicited by the mismatch in physical features between the standards and deviants but a violation of the regularity pattern shared among the standards. First, the EROS STC mismatch response was calculated by comparing brain responses to the same stimuli presented in different context (i.e., deviant minus control). The deviant events in the oddball blocks (i.e., IFC TMS, vertex TMS control, or auditory control blocks) were presented in a context with a constant pitch interval shared among the standards, while the physically identical control events in the equal probability control block were presented in a context with varying pitch intervals, in which the interval of the previous events could not establish a regular pattern or provide a predictive value for the next events. Second, the absolute pitches of the tone pairs varied among both the standard and deviant events. The regularity pattern or prediction could not be established based on the varying absolute pitches of the tones but the constant relative pitch differences. Third, although mismatch in physical features or sensory memories between the deviant and the preceding standard might exist in the oddball blocks, this mismatch would be identical to that between the control events of the deviants and the preceding filler events in the equal probability control block, as the pitch distributions of the tones were matched between the oddball blocks and the equal probability control block.

2.3 | Transcranial magnetic stimulation

The deviant stimuli were paired with TMS pulses produced by a monophasic single-pulse TMS stimulator (Neuro-MS/D, Neurosoft, Ivanovo, Russia) with an angulated 100-mm figure-of-eight coil. The TMS intensity was set to 80% of each participant's motor threshold. This TMS intensity level can produce a temporary functional disruption of the targeted brain region which abolishes the subsequent neural (Corthout, Uttl, Juan, Hallett, & Cowey, 2000; Tse et al., 2018) and behavioral responses (Davey, Romaguere, Maskill, & Ellaway, 1994). The motor threshold of the hand region in the right motor cortex for each participant was measured using the 5-cm rule method. At first, the TMS coil was positioned 5 cm to the right of the vertex, with a 45° orientation pointing toward the midline and tangential to the scalp surface. The location of the hand region was fine-tuned by moving the TMS coil along an imaginary grid with 1-cm steps. To search for the motor threshold, the intensity was first set at 30% of the stimulator's maximum output and increased by 5% in each step. The

resting motor threshold was determined by the minimum TMS intensity producing visible movement in any finger or the wrist in four out of eight consecutive trials.

A neural navigation system (Brain Science Tools BV, Utrecht, The Netherlands; <https://www.brainsciencetools.com/>) was used to monitor the TMS application on the right IFC and to locate the position of the EROS recording montage over the left STC in each participant (Figure 3b). The software Analysis of Functional NeuroImages (AFNI; Cox, 1996) was used to transform the Talairach coordinates of the target IFC and STC locations based on the previous studies (right IFC: $x = 60$, $y = 29$, $z = 14$; left STC: $x = -60$, $y = -27$, $z = 7$; Tse & Penney, 2008; Tse et al., 2013, 2015) to the native coordinates for each participant according to the individual's structural MRI. First, the structural MRI in native space was transformed to Talairach space to generate a native-to-Talairach space transformation matrix. Then, this transformation matrix was inverted and applied to reverse transform the coordinates of target IFC and STC locations from the Talairach space to the native space of each participant. The target coordinates in the native space of each participant were then entered into the neural navigator system for the TMS application and the EROS recordings. The stimulation intensity and the stimulation location were adjusted to reduce discomfort due to facial muscle twitches, jaw movements, or eyeblinks produced by TMS. However, the minimum stimulation intensity was higher than 75% of the motor threshold, and the stimulation location was maintained within 10 mm of the targeted IFC coordinates.

2.4 | EROS recording and analysis

The EROS recording and analysis procedure (summarized in Figure 1 of Tse, Gordon, Fabiani, & Gratton, 2010) was similar to that used in the previous TMS-EROS (Tse et al., 2018) and EROS MMN studies (Tse et al., 2006, 2013; Tse & Penney, 2007, 2008). Specifically, the EROS or fast optical signal was recorded using a frequency domain oximeter (Imagent, ISS, Inc., Champaign, IL). NIR light of 830 nm with intensity modulated at 110 MHz was emitted from laser diodes and carried by the plastic-clad silica optical fibers (2.5 m long; 400- μm diameter core) to the participants' scalps. The NIR light passing through the participants' scalps, skull, and brain was collected by fiber optic detector bundles and carried to the photomultiplier tubes (PMTs) of the oximeter. The signal passed to the PMT was mixed with a 110.003125 MHz signal to generate a signal with 3,125 Hz cross-correlational frequency. This output signal was sampled at 50 kHz by the analog-to-digital converter; then the digitized signal was fast-Fourier transformed to compute the DC intensity, AC intensity, and relative phase delay measures. Only phase delay data were analyzed in this study, as phase delay measure provides better sensitivity in measuring the EROS (Gratton et al., 2006). EROS was recorded from the left STC region with 8 light source and 16 detector fibers or a total of 128 source-detector pairs using a custom-built head-mount (Figure 3b). Each light source was turned on for 1.6 ms and time-multiplexed through the eight sources over a 12.8-ms period (i.e., 78.125 Hz).

Due to space limitations which made placing both the TMS coil and the EROS head mount on the right side of the head difficult, EROS was only measured on the left STC. Although it is possible to apply TMS to and record EROS from the same brain area using a low-profile head mount for optical fibers to reduce mechanical interference between the optical fibers with the TMS coil (Parks, 2013), there are drawbacks to this approach. The placement of the TMS coil limits the space for positioning the optical fibers and may sacrifice both the temporal and spatial resolution of the EROS measurements. To overcome these difficulties, TMS was applied to the right IFC, while the EROS was measured on the left STC. Previous studies have reported bilateral STC responses (Hsu et al., 2014; Liebenthal et al., 2003; Opitz et al., 2002; Rinne et al., 2005; Szycik, Stadler, Brechmann, & Münte, 2013; Tse et al., 2013; Tse & Penney, 2007) and right-dominant IFC responses (Doeller et al., 2003; Tse et al., 2013; Tse & Penney, 2007) in the preattentive detection of physical changes. EEG source localization studies have also reported the right IFC and the bilateral STC MMN generators in detecting abstract changes (Bendixen et al., 2008; Schröger et al., 2007).

The EROS data were coregistered with the $T - 1$ weighted structural MRI of each participant (Tse et al., 2010; Whalen, Maclin, Fabiani, & Gratton, 2008). The structural MRIs with preauricular and nasion points marked by Beekley Spots (Beekley Corporation, Bristol, CT) were recorded using a high-field 3.0-T whole-body scanner (Achieva TX, Philips Healthcare, Best, the Netherlands) with an eight-channel head coil. In each EROS session, a three-dimensional (3D) digitizer (Visor, ANT) was used to record the 3D locations of the fiducial points, the source and detector fibers, and 150 other points scattered around the scalp and ocular regions. The locations were coregistered with the MR anatomical data using a surface fitting method (Whalen et al., 2008). The locations of the source and detector fibers on the scalp were used to reconstruct the expected light path for each channel and participant in a common Talairach space (Talairach & Tournoux, 1988).

The optical data were corrected for phase wrapping, normalized, pulse corrected (Gratton & Corballis, 1995), and filtered with a 0.01–10-Hz band-pass filter. The filtered data were averaged for each time point, channel, condition, and participant, separately, using a 100-ms prestimulus baseline. The channels with a source–detector distance shorter than 20 mm or longer than 55 mm, or with phase variability (i.e., *SD* of a channel across trials and time points) greater than 160 ps were not included in the data analysis. The averaged data for each channel and each participant were reconstructed into the voxel space data and analyzed with Opt-3D software (Gratton, 2000). Specifically, the EROS for a given voxel was the average of the channels that overlapped at that particular voxel for each participant (Wolf et al., 2000), and *t* statistics were calculated across participants, for each voxel and each time point, and converted to *z* scores.

The statistical parametric map (SPM) of the EROS data was projected on a left lateral view of a template brain in Talairach space with an 8 mm full-width half-maximum (FWHM) spatial filter for each time point of 12.8 ms. Regions of interest (ROIs) and intervals of interest (IOIs) statistical analyses of the EROS data were based on previous

ERP studies on abstract change detection (Bendixen et al., 2008; Paavilainen, Arajärvi, & Takegata, 2007; Schröger et al., 2007) and previous EROS studies on physical change detection (Tse et al., 2006, 2013, 2018; Tse & Penney, 2007, 2008). The random field theory approach (Friston, Worsley, Frackowiak, Mazziotta, & Evans, 1994) was applied for multiple comparisons corrections. The *y* (anterior–posterior) and *z* (superior–inferior) Talairach coordinates were reported for the SPM with a lateral projection view.

SPM analyses were conducted on the EROS mismatch responses from 131 to 208 ms (Bendixen et al., 2008; Paavilainen et al., 2007; Schröger et al., 2007; Tse et al., 2006, 2013, 2018; Tse & Penney, 2007, 2008) after the onset of the second tone of the tone pair for both large and small deviants in the IFC TMS, vertex TMS control, and auditory control blocks. SPM analyses with one-sample *t* tests against zero were performed to examine the presence of the EROS mismatch responses in each condition. Two sets of interaction effect contrasts were separately conducted for the 80 and 200 ms pulse delays. The first contrast examined the difference in EROS mismatch response between the large and small deviants in the vertex TMS control and the auditory control blocks (vertex TMS – auditory control contrast in Table 1). The second contrast examined whether the average of the EROS mismatch responses difference between the large and small deviants in the vertex TMS control and auditory control blocks is larger than the EROS mismatch response difference between the large and small deviants in the IFC TMS block ([vertex TMS + auditory control] – IFC TMS contrast in Table 1). When both interaction effect contrasts were not statistically significant, a main effect contrast was conducted to examine whether the averaged EROS mismatch responses to the large deviants were larger than those to small deviants across the IFC TMS, vertex TMS control, and auditory control blocks.

In addition to the SPM analyses, repeated measures analysis of variance (ANOVA) with the factors deviance level (small and large), block type (IFC TMS, vertex TMS control, and auditory control), and TMS pulse delay (80 and 200 ms) was conducted on the peak EROS STC mismatch responses within the ROI and IOI of each condition. Follow-up repeated measures ANOVAs and paired *t* tests (two tailed) were performed to compare the differences in the EROS STC mismatch responses to large and small deviants among the block types and TMS pulse delays. The Greenhouse–Geisser correction, with the epsilon (ϵ) correction factor, was applied when appropriate.

3 | RESULTS

EROS STC responses from 131 to 208 ms after the onset of the second tone projected onto the left lateral view of a template brain are shown in Figure 4. Consistent with our prediction, no statistically significant STC mismatch response was elicited by the large deviant when TMS was applied to the IFC with an 80 ms delay after the onset of the second tone. However, significant STC mismatch responses (Brodmann area 21 and 22) to large deviants were found in the vertex TMS control and auditory control blocks when the TMS pulse was

TABLE 1 Contrast weights for SPM analyses

		Vertex TMS – auditory control ^a		(Vertex TMS + auditory control) – IFC TMS ^b		Large – small ^c	
		Small	Large	Small	Large	Small	Large
Block type	IFC TMS	0	0	1/2	-1/2	-1/3	1/3
	Vertex TMS control	-1/2	1/2	-1/4	1/4	-1/3	1/3
	Auditory control	1/2	-1/2	-1/4	1/4	-1/3	1/3

Abbreviations: IFC, inferior frontal cortex; SPM, statistical parametric map; TMS, transcranial magnetic stimulation.

^a(Large – small) in vertex TMS control – (large – small) in auditory control.

^b[(Large – small) in vertex TMS control + (large – small) in auditory control]/2 – (large – small) in IFC TMS.

^c(Large – small) in IFC TMS + (large – small) in vertex TMS control + (large – small) in auditory control/3.

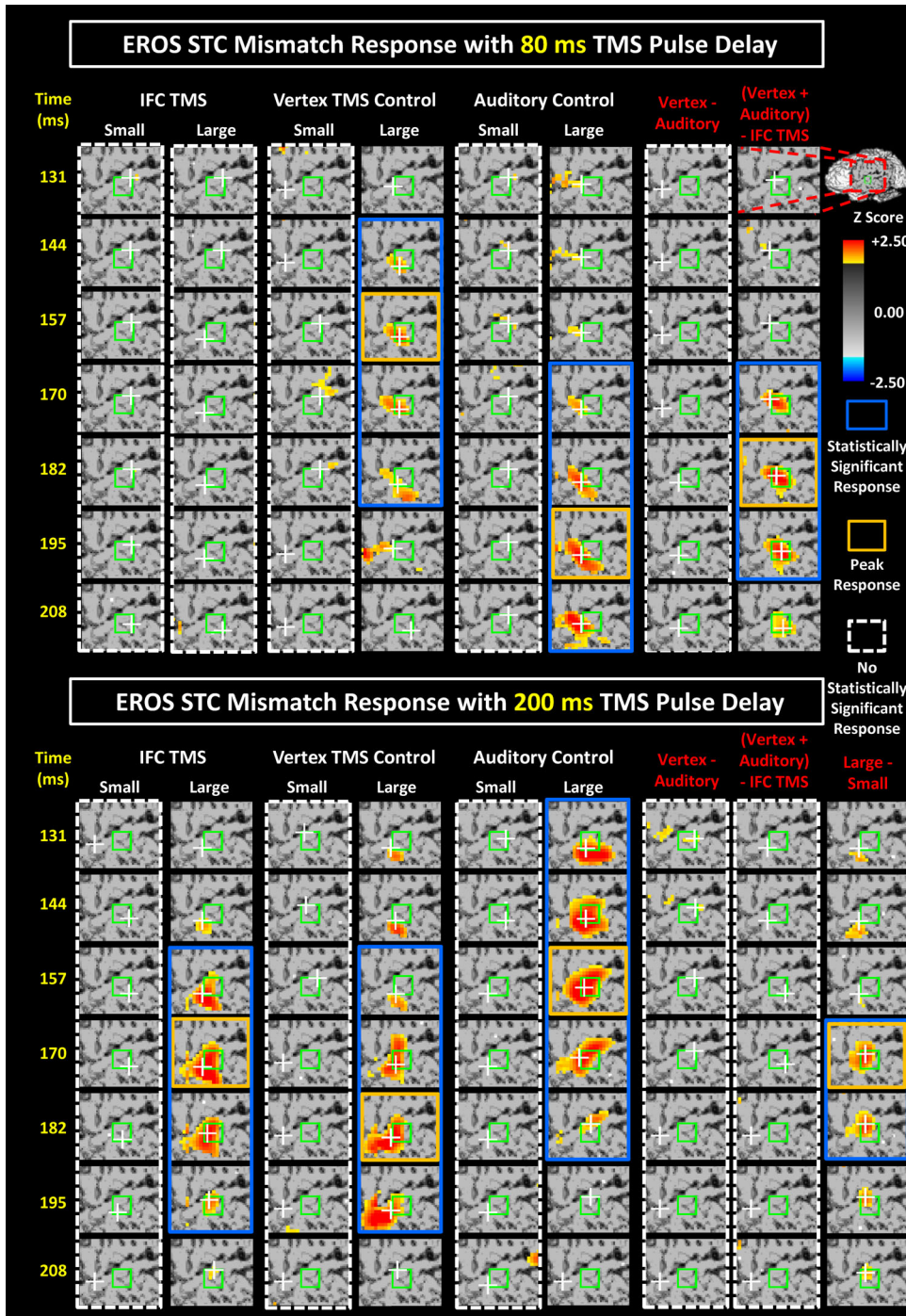


FIGURE 4 Statistical maps of the EROS STC mismatch responses projected onto left lateral views of a template brain. The upper and lower panels demonstrate the results for conditions with 80 and 200 ms TMS pulse delays, respectively. The darker gray color marked on the template brain represents the EROS recording regions covered by the optical montage. The green box indicates the ROI, and the white cross indicates the location of the peak EROS response. EROS, event-related optical signal; STC, superior temporal cortex; TMS, transcranial magnetic stimulation; ROI, region of interest

applied with an 80 ms delay. Significant STC mismatch responses to large deviants were also found in the IFC TMS, vertex TMS control, and auditory control blocks when the TMS pulse was applied with a 200 ms delay. No mismatch response was found for the small deviants in any of the blocks with 80 or 200 ms TMS pulse delay. The Z scores, critical Z values, latencies, and Talairach coordinates of the peak EROS STC mismatch responses are shown in Table 2.

The interaction contrast comparing the difference in EROS STC mismatch responses to the difference of the large and small deviants between the IFC TMS block and the averaged vertex TMS and auditory control blocks was statistically significant when TMS pulses were applied with 80 ms delay, but not with 200 ms delay. The interaction effect contrast comparing the EROS mismatch response difference of the large and small deviants between the vertex TMS control and auditory control blocks was not statistically significant for TMS pulse delay of 80 or 200 ms. The contrast comparing the EROS STC mismatch responses to the large and small deviants averaged across the IFC TMS, vertex TMS control, and auditory control blocks was statistically significant for the 200 ms delay but not the 80 ms TMS pulse delay condition (Table 3).

Repeated measures ANOVA, with the factors deviance level (large and small), block type (IFC TMS, vertex TMS control, and auditory control), and TMS pulse delay (80 and 200 ms) was conducted on the peak EROS STC mismatch responses extracted from each condition (Figure 5). The main effects of deviance level ($F[1, 23] = 3.86$, $p = .06$), block type ($F[2, 23] = 0.88$, $p = .42$), and TMS pulse delay ($F[1, 23] = 0.56$, $p = .46$), as well as the two-way interactions between deviance level and block type ($F[2, 46] = 1.12$, $p = .33$), between block type and TMS pulse delay ($F[2, 46] = 1.18$, $p = .31$), and between deviance level and TMS pulse delay ($F[1, 23] = 2.12$, $p = .16$) were not statistically significant. However, the three-way interaction of deviance level, block type, and TMS pulse delay was significant ($F[2, 46] = 3.62$, $p = .040$, partial eta square, $\eta_p^2 = 0.14$). Follow-up repeated measures ANOVAs, with the factors deviance level (large and small) and block type (IFC TMS, vertex TMS control, and auditory control) were conducted separately for the peak responses in the 80 and 200 ms pulse delay conditions.

For the 80 ms TMS pulse delay condition, the main effects of deviance level ($F[1, 23] = 0.65$, $p = .43$) and block type ($F[2, 46] = 1.12$, $p = .34$) were not statistically significant. However, the interaction effect of deviance level and block type was significant ($F[2, 46] = 4.20$, $p = .021$, $\eta_p^2 = 0.15$). Follow-up one-way repeated measures ANOVAs showed significant difference in the EROS STC mismatch responses to the large deviant among the three block types ($F[2, 46] = 5.19$, $p = .018$, $\eta_p^2 = 0.18$) but not to the small deviants among the three block types ($F[2, 46] = 0.08$, $p = .92$). Follow-up paired-wise comparisons with *t* tests showed significant differences in the EROS STC mismatch responses to the large deviants between IFC TMS block and vertex TMS control block ($t[23] = 3.91$, $p < .001$, Cohens' *d* [hereafter *d*] = .80) and between IFC TMS block and auditory control block ($t(23) = 2.52$, $p = .018$, $d = .52$), but not for the difference between vertex TMS control block and auditory control block ($t[23] = -0.50$, $p = .10$). For the 200 ms TMS pulse delay condition, significant main effect of deviance level was observed ($F[1, 23] = 4.76$, $p = .040$, $\eta_p^2 = .17$), while the main effects of block type ($F[2, 46] = 0.99$, $p = .36$), and interaction effect of deviance level and block type ($F[2, 46] = 0.11$, $p = .89$) were not statistically significant.

Both the SPM analyses and peak EROS mismatch response analyses demonstrate that the IFC at the predetection stage served a critical functional role in eliciting the later STC mismatch responses when deviants violated an abstract rule established by the standard events. The differences in EROS STC mismatch responses between the IFC TMS and vertex TMS control blocks and between the 80 and 200 ms TMS pulse delay conditions established the spatial and temporal specificity of the TMS effects, respectively. In addition, the comparison between the IFC TMS and auditory control blocks demonstrates that the IFC TMS effect on the STC mismatch response cannot be attributed merely to the difference in TMS pulse noise between standard and deviant stimuli.

The peak latencies of STC mismatch responses were not statistically different among the 80 ms TMS pulse delay conditions ($F[1, 23] = 0.71$, $p = .71$), the 200 ms TMS pulse delay conditions ($F[2, 46] = 0.81$, $p = .45$), or among all five conditions with a significant STC mismatch responses ($F[4, 92] = 0.93$, $p = .44$). This result is kind

TABLE 2 EROS mismatch responses at STC

Block type Deviance magnitude	IFC TMS		Vertex TMS control		Auditory control	
	Small	Large	Small	Large	Small	Large
TMS pulse delay	80 ms					
Peak Z (critical Z)	0.92 (1.64)	0.50 (2.13)	1.02 (1.82)	2.56* (2.36)	0.68 (1.64)	2.62* (2.19)
Peak latency (ms)	157	157	170	157	170	195
Talairach coordinate (y, z)	-26, 9	-13, -3	-26, 9	-18 -1	-26, 9	-13, -1
TMS pulse delay	200 ms					
Peak Z (critical Z)	0.50 (1.64)	2.89* (2.20)	0.14 (1.79)	2.86* (2.23)	1.22 (1.96)	2.94* (2.10)
Peak latency (ms)	182	170	157	182	182	157
Talairach coordinate (y, z)	-21, -3	-13, -3	-26, 9	-13, -1	-13, -3	-16, 2

Abbreviations: EROS, event-related optical signal; IFC, inferior frontal cortex; STC, superior temporal cortex; TMS, transcranial magnetic stimulation.
Note: Asterisk (*) indicates peak Z > Critical Z with $p < .05$, with corrections for multiple comparisons.

TABLE 3 Contrast analyses of the peak STC mismatch responses

Contrast	Vertex TMS - auditory control	(Vertex TMS + auditory control) - IFC TMS	Large - small
TMS pulse delay	80 ms		
Peak Z (critical Z)	0.81 (1.64)	2.69* (2.58)	1.65 (1.86)
Peak latency (ms)	208	182	170
Talairach coordinate (y, z)	-14, -1	-18, 4	-14, -3
TMS pulse delay	200 ms		
Peak Z (critical Z)	1.21 (1.91)	1.03 (1.94)	2.46* (2.41)
Peak latency (ms)	157	157	170
Talairach coordinate (y, z)	-28, 4	-28, 2	-18, 7

Abbreviations: IFC, inferior frontal cortex; STC, superior temporal cortex; TMS, transcranial magnetic stimulation.

Note: Asterisk (*) indicates peak Z > Critical Z with $p < .05$, with corrections for multiple comparisons.

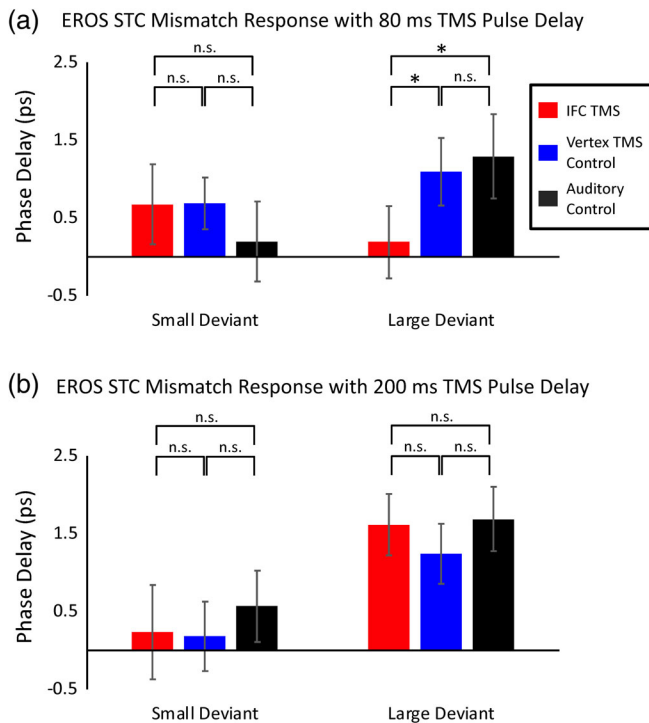


FIGURE 5 Peak amplitude of the averaged EROS mismatch response within the region and interval of interest to the large and small deviants in the IFC TMS, vertex TMS control, and auditory control blocks. The upper and lower panels show the results for TMS with 80- and 200-ms delay. Error bars indicate the SEM-computed across participants. * $p < .05$. EROS, event-related optical signal; n.s., nonsignificant difference; TMS, transcranial magnetic stimulation

of expected as statistically significant STC mismatch responses were consistently found at 170 and 182 ms for the 80 ms TMS pulse delay conditions and at 157, 170, and 182 ms for the 200 ms TMS pulse delay conditions (highlighted in blue frames in Figure 4). Although the peak latencies of the STC mismatch responses were not aligned at the same time/data point, the peak responses were measured from the same STC mismatch response, which is typically observed in previous EROS studies (Tse et al., 2006, 2013, 2018).

4 | DISCUSSION

The present study investigated the functional connectivity between the IFC and the STC in the preattentive detection of abstract rule violation by perturbing the functioning of the IFC at the predetection stage with TMS and observing the later STC mismatch response with EROS. A pitch interval rule was established by maintaining a constant relative pitch difference between the tones of the standard tone pairs, while the absolute pitches of the tones were allowed to vary. Deviant tone pairs were different from the standard tone pairs by reduced relative pitch differences that violated the pitch interval rule. When a TMS pulse was applied on the IFC at 80 ms after the deviance onset, the EROS STC mismatch response to large deviant was abolished. However, the STC mismatch responses to large deviants were consistently observed when TMS was applied to the IFC at 200 ms, or when sham TMS at vertex or TMS sound recording was delivered at 80 and 200 ms. These results extend the findings of our previous TMS-EROS study (Tse et al., 2018) demonstrating a critical functional role of the IFC for the later STC mismatch response from the preattentive detection of physical change to the detection of abstract change or abstract rule violation and provide support for a generic frontotemporal network in preattentive change detection suggested in the regularity violation hypothesis (Winkler, 2007) and the predictive coding perspective of the mismatch response (Friston, 2005, 2010; Garrido et al., 2007).

A common predictive mechanism is hypothesized in the preattentive detection of both physical and abstract changes in the regularity violation hypothesis (Winkler, 2007) and under the predictive coding framework (Friston, 2005, 2010; Garrido et al., 2007). The regularity violation hypothesis suggests that the regularity in the acoustic environment is extracted for predicting future events (Winkler, 2007; Winkler & Schröger, 2015). The predictive coding account further proposes a forward and backward circuit between the IFC and the STC underlying the prediction mechanism. Although our earlier study (Tse et al., 2018) demonstrated the critical role of the IFC in eliciting the STC mismatch responses to physical change, the mismatch response to physical change can be triggered by the mismatch in physical features between the deviant and the standard events or by violating the

prediction or regularity pattern (Winkler & Schröger, 2015). It remains inconclusive if the regularity among the standard events is extracted for making predictions of future events and detecting events deviating from the prediction. To address this issue, the current study adopted a passive oddball paradigm in which the absolute pitches of the standard tone pairs varied, while the relative pitch differences among the standard tone pairs were kept constant. The regularity pattern could only be extracted from the relative pitch difference (i.e., an abstract feature) among the standard events, but not from the varying absolute pitch (i.e., a physical feature), in the change detection process to elicit the mismatch response.

In addition, the differences in physical features between the deviant and the standard in the IFC TMS, vertex TMS control, and auditory control blocks, and between the control for deviant events and the filler events in the equal probability control block were similar. Comparisons between the deviants in the IFC TMS, vertex TMS control, and auditory control blocks and the control for deviants in the equal probability control block would produce null differences. Thus, the EROS STC mismatch response observed could only be explained by the regularity or prediction violation, but not differences in the physical features of the events.

The IFC and STC are suggested to be hierarchically organized with forward and backward functional connections for building the predictive model (Garrido et al., 2007; Garrido, Kilner, Kiebel, & Friston, 2008; Gratton, 2018). Dynamic causal modeling of the MMN responses to pitch change demonstrated better model fit at 200 ms after the deviance onset with both forward (bottom-up) connection from the STC to the IFC generator and the backward (top-down) connection from the IFC to the STC than the model with the forward connection only (Garrido et al., 2007). The backward connection was hypothesized to be important for updating the predictive model in the IFC (Friston, 2012). The disruptive IFC TMS effect at 80 ms on the later STC mismatch responses in the current study demonstrated an earlier IFC-to-STC top-down connection which may indicate the recall of the regularity pattern, the activation of the prediction model, and/or the transfer of the prediction information for change detection in the STC. The TMS effect may also indicate the involvement of the recursive forward and backward IFC-STC connection as early as 80 ms. The difference in the latency of the IFC-to-STC connection in the EEG/ERP modeling studies (e.g., Garrido et al., 2007) and the TMS-EROS studies can be explained by the difference in neuronal signals measured by these brain imaging methods. EEG/ERP is more sensitive to the neuronal signals of the pyramidal cells, while EROS is more sensitive to the neuronal signals of the smaller interneuron (Gratton & Fabiani, 2009). Previous studies with simultaneous EEG/ERP and EROS recording had demonstrated both similarities and differences in the ERP N200, P300, N400, P600, and MMN and their EROS counterparts (Tse et al., 2013, 2015; Tse, Low, Fabiani, & Gratton, 2012; Tse & Penney, 2007, 2008). Future studies can delineate the time course of the recursive circuit by stimulating and recording the brain responses at both the IFC and the STC. Earlier studies have demonstrated an IFC-to-STC followed by IFC mismatch response pattern in the pre-attentive change detection process

(e.g., Tse et al., 2013). By applying TMS on the IFC 80 ms or on the STC 150 ms after deviant onset, and recording the STC at 150 ms and the IFC after 200 ms with EROS, we could examine the connection of the early IFC-to-STC, and the STC-to-late IFC recursive connections of the frontotemporal network. TMS on the early IFC or the STC would abolish the subsequent brain responses in the recursive circuit.

The current study provides evidence for the functional connectivity between the IFC and the STC in the preattentive abstract change detection, which is assumed by the prediction model hypotheses (Friston, 2005, 2010; Garrido et al., 2007; Winkler, 2007). However, this result could not eliminate nonmutually exclusive alternative explanations such as the contrast enhancement hypothesis (Opitz et al., 2002) which also assumes the IFC's involvement in the stimulus analysis process before the change detection response occurs in the STC. Specifically, the IFC is involved in amplifying the difference between the deviant and the standard/prediction when the difference is small or ambiguous. This hypothesis was first developed based on the results on physical change detection and did not predict the brain responses to abstract changes. However, as physical and abstract changes are not independent, it is possible that the same mechanism could be involved in detecting both physical and abstract changes. In general, changes in abstract properties are less salient compared to changes in physical properties. In physical change detection, a smaller change would require stronger contrast enhancement (i.e., indicated by the IFC mismatch response) than a larger change. However, in abstract change detection, a large change may also require the contrast enhancement process, while a small change may not be able to initiate the contrast enhancement process. Based on these predictions, our findings are also in line with the contrast enhancement hypothesis.

The functional role of the IFC in detecting abstract changes was concluded based on the abolishment of the STC mismatch response produced by the disruptive TMS effect. However, in addition to the TMS effect, the absence of brain responses could be driven by incorrect stimulation location and/or latency, weak stimulation intensity, or the lack of statistical power (de Graaf & Sack, 2011). To address these issues and ensure a valid interpretation of the results, we applied the experimental design and analysis procedures adopted in our previous TMS-EROS study (Tse et al., 2018) which was recommended by de Graaf and Sack (2011). The target IFC TMS location and latency were selected based on previous EROS studies (Tse et al., 2006, 2013; Tse & Penney, 2007, 2008) and the TMS-EROS study (Tse et al., 2018). The TMS location was identified and monitored during the experiment by using the neural navigation system with the structural MRI of individual participant. The stimulation locations were maintained within a 10-mm radius of the targeted location. Several experimental control conditions were incorporated into the current design to ensure the spatial, temporal, and functional specificity of the TMS effect. The conclusion of a disruptive effect of IFC TMS was drawn from comparisons between the EROS responses in the IFC TMS block with those in the control conditions. First, the vertex TMS control block served as a control for the TMS location to establish the spatial specificity of the TMS effect. Second, the 200 ms TMS delay

condition was designed to establish the temporal specificity of the IFC TMS effect. With this temporal control, the effects of the IFC TMS applied with an 80 ms delay cannot be attributed to general brain activity changes triggered by the energy from the TMS pulse. Third, the auditory control block was included as the baseline condition to show that the STC mismatch response can be elicited without the application of TMS to the brain but in a similar auditory environment. Fourth, the modulation of the STC mismatch responses by deviance level demonstrated that the cognitive function implicated by the brain response is abolished by the TMS on the IFC. Last, the STC mismatch responses were repeatedly observed in multiple control conditions in both the current and our previous TMS-EROS study (Tse et al., 2018), the absence of the STC mismatch response to the deviants in the IFC TMS block is not likely to be driven by insufficient statistical power.

The small-deviant conditions were included in this study to provide a contrast of the STC mismatch responses between small and large deviant conditions within each block type. The small deviant conditions served as a cognitive control condition to exclude possible confounds due to the auditory and somatosensory sensations induced by a specific TMS effect (e.g., TMS on the IFC). If the STC mismatch responses were elicited by the sensory effects produced by the TMS pulse or TMS sound recording, but not prediction violation, the STC mismatch responses to both large and small conditions of the same block type would be identical. Ideally, the STC mismatch responses elicited by the small deviant conditions should be smaller than the large deviant conditions, and statistically different from zero, in all the conditions except for the IFC TMS with 80 ms delay condition. To produce this ideal pattern, the deviance level has to be carefully selected based on the results of previous or pilot studies, but such information is not available in the literature to our best knowledge. Although the current study found non-significant mismatch responses to the small deviants in all the conditions, the differences in STC mismatch responses between the large and small deviant conditions provide the evidence to exclude possible confounds due to the sensory responses induced by TMS, and to interpret the STC mismatch response as a brain response specific to prediction violation by the large deviant.

To control for the sensory effects produced by the TMS pulse, it is logical to pair both deviants and standards with TMS on the IFC. However, as suggested by the prediction violation account, the IFC may also be involved in extracting the regularity among the standards for building a prediction model, pairing the standards with TMS on the IFC may also disrupt these processes lead to the absence of STC mismatch responses to the deviants. Our recent study (Lui et al., in review) showed that pairing the initial two standards in a train of standards with TMS on the IFC with 80 ms delay would abolish later mismatch responses to deviants. Considering the possible disruptive TMS effect on processing the standards, we should be cautious about introducing TMS pulses on the standards.

In the TMS-EROS study on preattentive detection of physical change (Tse et al., 2018), significant mismatch responses were observed in deviants preceded by 4–7 standards. However, significant mismatch responses were only observed in deviants preceded by 6–7 standards in

the current study. The difference in the number of standards preceding the deviant eliciting the STC mismatch responses in the two studies could be driven by the differences in the abstractness of the regularity pattern embedded in the standard events. The current study adopted the pitch interval rule which required a longer standard train to provide sufficient rule-conforming information to establish the regularity pattern. Modulation of mismatch responses by standard train length was also found in previous studies. For example, a pitch change preceded by 2–3 standards could elicit a significant MMN (Bendixen, Roeber, & Schröger, 2007), while a change in the contingency between pitch and duration of a tone only elicited MMN responses when preceded by a train with at least 15 standards (Bendixen et al., 2008).

A direct structural connection between the right IFC and the left STC is not required for the functional connectivity argument in the current study. Studies using diffusion tensor imaging have revealed the structural connections between the IFC and the STC (Frühholz & Grandjean, 2013) and between bilateral temporal cortices (Hofer & Frahm, 2006). It is possible that the functional connection between the right IFC and the left STC is mediated through the right STC or another brain region. With the TMS applied on the IFC at an earlier stage and the abolishment of later STC mismatch response, the functional connectivity of the IFC leading to the STC mismatch responses could be established.

In summary, the current study made use of the superior spatio-temporal localization abilities of both TMS and EROS, and the absence of electromagnetic inference between the two techniques to investigate the functional connectivity between the IFC and the STC in abstract change detection. The results demonstrated a disruptive IFC TMS effect on the later STC mismatch response to the violation of a pitch interval rule, and provided evidence for a directional functional connectivity between the IFC and the STC in the abstract change detection. The consistent IFC–STC connection revealed in the current study and our previous study (Tse et al., 2018) provided support for a generic frontotemporal network suggested by the prediction violation account of preattentive change detection.

ACKNOWLEDGMENTS

Part of this work was completed by X.-Z. Xiao in partial fulfillment of the requirement for a Ph.D. degree at The Chinese University of Hong Kong. We wish to thank Lydia Yee for helpful comments on earlier versions of this manuscript. This project was supported by funding from the General Research Fund of the Research Grants Council (14606417) awarded to C.-Y. Tse by the of the Hong Kong SAR University Grants Committee.

CONFLICT OF INTERESTS

S. F. W. Neggers is the owner of Brain Science Tools BV. The authors declare no conflict of interest otherwise.

DATA AVAILABILITY STATEMENT

The data that support the findings of this study are available upon reasonable request. Restrictions apply to the availability of these data, with the permission of the funding agency.

ORCID

Chun-Yu Tse  <https://orcid.org/0000-0002-6120-2971>

REFERENCES

- Bendixen, A., Prinz, W., Horváth, J., Trujillo-Barreto, N. J., & Schröger, E. (2008). Rapid extraction of auditory feature contingencies. *NeuroImage*, 41(3), 1111–1119. <https://doi.org/10.1016/j.neuroimage.2008.03.040>
- Bendixen, A., Roeber, U., & Schröger, E. (2007). Regularity extraction and application in dynamic auditory stimulus sequences. *Journal of Cognitive Neuroscience*, 19, 1664–1677. <https://doi.org/10.1162/jocn.2007.19.10.1664>
- Bidelman, G. M., & Chung, W. L. (2015). Tone-language speakers show hemispheric specialization and differential cortical processing of contour and interval cues for pitch. *Neuroscience*, 305, 384–392. <https://doi.org/10.1016/j.neuroscience.2015.08.010>
- Brainard, D. H. (1997). The psychophysics toolbox. *Spatial Vision*, 10(4), 433–436. <https://doi.org/10.1163/156856897X00357>
- Caclin, A., Brattico, E., Tervaniemi, M., Näätänen, R., Morlet, D., Giard, M.-H., & McAdams, S. (2006). Separate neural processing of timbre dimensions in auditory sensory memory. *Journal of Cognitive Neuroscience*, 18(12), 1959–1972. <https://doi.org/10.1162/jocn.2006.18.12.1959>
- Corthout, E., Uttl, C. A. B., Juan, C., Hallett, M., & Cowey, A. (2000). Suppression of vision by transcranial magnetic stimulation: A third mechanism. *NeuroImage*, 11(11), 2345–2349.
- Cox, R. W. (1996). AFNI: Software for analysis and visualization of functional magnetic resonance neuroimages. *Computers and Biomedical Research*, 29(29), 162–173.
- Davey, N. J., Romaiguere, P., Maskill, D. W., & Ellaway, P. H. (1994). Suppression of voluntary motor activity revealed using transcranial magnetic stimulation of the motor cortex in man. *The Journal of Physiology*, 477(2), 223–235. <https://doi.org/10.1113/jphysiol.1994.sp020186>
- de Graaf, T. A., & Sack, A. T. (2011). Null results in TMS: From absence of evidence to evidence of absence. *Neuroscience and Biobehavioral Reviews*, 35(3), 871–877. <https://doi.org/10.1016/j.neubiorev.2010.10.006>
- Denham, S. L., Gyimesi, K., Stefanics, G., & Winkler, I. (2013). Perceptual bistability in auditory streaming: How much do stimulus features matter? *Learning & Perception*, 5(Supplement 2), 73–100. <https://doi.org/10.1556/LP.5.2013.Supp2.6>
- Doeller, C. F., Opitz, B., Mecklinger, A., Krick, C., Reith, W., & Schröger, E. (2003). Prefrontal cortex involvement in preattentive auditory deviance detection: Neuroimaging and electrophysiological evidence. *NeuroImage*, 20(2), 1270–1282. [https://doi.org/10.1016/S1053-8119\(03\)00389-6](https://doi.org/10.1016/S1053-8119(03)00389-6)
- Dürschmid, S., Edwards, E., Reichert, C., Dewar, C., Hinrichs, H., Heinze, H.-J., ... Knight, R. T. (2016). Hierarchy of prediction errors for auditory events in human temporal and frontal cortex. *Proceedings of the National Academy of Sciences*, 113(24), 201525030. <https://doi.org/10.1073/pnas.1525030113>
- Friston, K. J. (2005). A theory of cortical responses. *Philosophical Transactions of the Royal Society of London. Series B, Biological Sciences*, 360(1456), 815–836. <https://doi.org/10.1098/rstb.2005.1622>
- Friston, K. J. (2010). The free-energy principle: A unified brain theory? *Nature Reviews Neuroscience*, 11(2), 127–138. <https://doi.org/10.1038/nrn2787>
- Friston, K. J. (2011). Functional and effective connectivity: A review. *Brain Connectivity*, 1(1), 13–36. <https://doi.org/10.1089/brain.2011.0008>
- Friston, K. J. (2012). Prediction, perception and agency. *International Journal of Psychophysiology*, 83(2), 248–252. <https://doi.org/10.1016/j.ijpsycho.2011.11.014>
- Friston, K. J., Worsley, K. J., Frackowiak, R. S. J., Mazziotta, J. C., & Evans, A. C. (1994). Statistical parametric maps in functional imaging: A general linear approach. *Human Brain Mapping*, 1(3), 210–220. <https://doi.org/10.1002/hbm.460010306>
- Frühholz, S., & Grandjean, D. (2013). Processing of emotional vocalizations in bilateral inferior frontal cortex. *Neuroscience and Biobehavioral Reviews*, 37(10), 2847–2855. <https://doi.org/10.1016/j.neubiorev.2013.10.007>
- Garrido, M. I., Kilner, J. M., Kiebel, S. J., & Friston, K. J. (2007). Evoked brain responses are generated by feedback loops. *Proceedings of the National Academy of Sciences of the United States of America*, 104(52), 20961–20966. <https://doi.org/10.1073/pnas.0706274105>
- Garrido, M. I., Kilner, J. M., Kiebel, S. J., & Friston, K. J. (2008). Dynamic causal modeling of the response to frequency deviants. *Journal of Neurophysiology*, 101(5), 2620–2631. <https://doi.org/10.1152/jn.90291.2008>
- Gratton, G. (2018). Brain reflections: A circuit-based framework for understanding information processing and cognitive control. *Psychophysiology*, 55(3), 1–26. <https://doi.org/10.1111/psyp.13038>
- Gratton, G. (2000). "Opt-cont" and "opt-3D": A software suite for the analysis and 3D reconstruction of the event-related optical signal (EROS). In *Psychophysiology* (Vol. 37, pp. S44–S44). New York, NY: Cambridge University Press.
- Gratton, G., Brumback, C. R., Gordon, B. A., Pearson, M. A., Low, K. A., & Fabiani, M. (2006). Effects of measurement method, wavelength, and source-detector distance on the fast optical signal. *NeuroImage*, 32(4), 1576–1590. <https://doi.org/10.1016/j.neuroimage.2006.05.030>
- Gratton, G., & Corballis, P. M. (1995). Removing the heart from the brain: Compensation for the pulse artifact in the photon migration signal. *Psychophysiology*, 32(3), 292–299. <https://doi.org/10.1111/j.1469-8986.1995.tb02958.x>
- Gratton, G., & Fabiani, M. (2001). Shedding light on brain function: The event-related optical signal. *Trends in Cognitive Sciences*, 5(8), 357–363. [https://doi.org/10.1016/S1364-6613\(00\)01701-0](https://doi.org/10.1016/S1364-6613(00)01701-0)
- Gratton, G., & Fabiani, M. (2009). Fast optical signals: Principles, methods, and experimental results. In R. Frostig (Ed.), *In Vivo Optical Imaging of Brain Function* (2nd ed., pp. 435–460). Boca Raton, FL: CRC Press.
- Hofer, S., & Frahm, J. (2006). Topography of the human corpus callosum revisited-comprehensive fiber tractography using diffusion tensor magnetic resonance imaging. *NeuroImage*, 32(3), 989–994. <https://doi.org/10.1016/j.neuroimage.2006.05.044>
- Hsu, C. H., Lin, S. K., Hsu, Y. Y., & Lee, C. Y. (2014). The neural generators of the mismatch responses to Mandarin lexical tones: An MEG study. *Brain Research*, 1582, 154–166. <https://doi.org/10.1016/j.brainres.2014.07.023>
- Jacobsen, T., & Schröger, E. (2001). Is there pre-attentive memory-based comparison of pitch? *Psychophysiology*, 38(4), 723–727. <https://doi.org/10.1017/s0048577201000993>
- Kiebel, S. J., Garrido, M. I., Moran, R., Chen, C. C., & Friston, K. J. (2009). Dynamic causal modeling for EEG and MEG. *Human Brain Mapping*, 30(6), 1866–1876. <https://doi.org/10.1002/hbm.20775>
- Korzyukov, O. A., Winkler, I., Gumenyuk, V. I., & Alho, K. (2003). Processing abstract auditory features in the human auditory cortex. *NeuroImage*, 20(4), 2245–2258. <https://doi.org/10.1016/j.neuroimage.2003.08.014>
- Lappe, C., Steinsträter, O., & Pantev, C. (2013). Rhythmic and melodic deviations in musical sequences recruit different cortical areas for mismatch detection. *Frontiers in Human Neuroscience*, 7(June), 1–9. <https://doi.org/10.3389/fnhum.2013.00260>
- Liebenthal, E., Ellingson, M. L., Spanaki, M. V., Prieto, T. E., Ropella, K. M., & Binder, J. R. (2003). Simultaneous ERP and fMRI of the auditory cortex in a passive oddball paradigm. *NeuroImage*, 19(4), 1395–1404. [https://doi.org/10.1016/S1053-8119\(03\)00228-3](https://doi.org/10.1016/S1053-8119(03)00228-3)
- Lui, T. K.-Y., Shum, Y.-H., Xiao, X.-Z., Wang, Y., Cheung, A. T.-C., Chan, S. S.-M., Neggers, S. F. W., & Tse, C.-Y. (2020). The Critical Role of the Inferior Frontal Cortex in Establishing a Prediction Model for Generating Subsequent Mismatch Negativity (MMN): A TMS-EEG Study (in review).

- MacLean, S. E., Blundon, E. G., & Ward, L. M. (2015). Brain regional networks active during the mismatch negativity vary with paradigm. *Neuropsychologia*, 75, 242–251. <https://doi.org/10.1016/j.neuropsychologia.2015.06.019>
- May, P. J. C., & Tiitinen, H. (2010). Mismatch negativity (MMN), the deviance-elicited auditory deflection, explained. *Psychophysiology*, 47(1), 66–122. <https://doi.org/10.1111/j.1469-8986.2009.00856.x>
- Mittag, M., Takegata, R., & Winkler, I. (2016). Transitional probabilities are prioritized over stimulus/pattern probabilities in auditory deviance detection: Memory basis for predictive sound processing. *Journal of Neuroscience*, 36(37), 9572–9579. <https://doi.org/10.1523/JNEUROSCI.1041-16.2016>
- Molholm, S., Martinez, A., Ritter, W., Javitt, D. C., & Foxe, J. J. (2005). The neural circuitry of pre-attentive auditory change-detection: An fMRI study of pitch and duration mismatch negativity generators. *Cerebral Cortex*, 15(5), 545–551. <https://doi.org/10.1093/cercor/bhh155>
- Näätänen, R., & Michie, P. T. (1979). Early selective-attention effects on the evoked potential: A critical review and reinterpretation. *Biological Psychology*, 8(2), 81–136. [https://doi.org/10.1016/0301-0511\(79\)90053-X](https://doi.org/10.1016/0301-0511(79)90053-X)
- Näätänen, R., Paavilainen, P., Alho, K., Reinikainen, K., & Sams, M. (1989). Do event-related potentials reveal the mechanism of the auditory sensory memory in the human brain? *Neuroscience Letters*, 98(2), 217–221. [https://doi.org/10.1016/0304-3940\(89\)90513-2](https://doi.org/10.1016/0304-3940(89)90513-2)
- Näätänen, R., Paavilainen, P., Rinne, T., & Alho, K. (2007). The mismatch negativity (MMN) in basic research of central auditory processing: A review. *Clinical Neurophysiology*, 118(12), 2544–2590. <https://doi.org/10.1016/j.clinph.2007.04.026>
- Näätänen, R., & Winkler, I. (1999). The concept of auditory stimulus representation in neuroscience. *Psychological Bulletin*, 125(6), 826–859.
- Nyffeler, T., Hartmann, M., Hess, C. W., & Müri, R. M. (2008). Visual vector inversion during memory antisaccades—A TMS study. *Progress in Brain Research*, 171(08), 429–432. [https://doi.org/10.1016/S0079-6123\(08\)00663-8](https://doi.org/10.1016/S0079-6123(08)00663-8)
- Oldfield, R. C. (1971). The assessment and analysis of handedness: The Edinburgh inventory. *Neuropsychologia*, 9(1), 97–113. [https://doi.org/10.1016/0028-3932\(71\)90067-4](https://doi.org/10.1016/0028-3932(71)90067-4)
- Opitz, B., Rinne, T., Mecklinger, A., von Cramon, D. Y., & Schröger, E. (2002). Differential contribution of frontal and temporal cortices to auditory change detection: fMRI and ERP results. *NeuroImage*, 15(1), 167–174. <https://doi.org/10.1006/nimg.2001.0970>
- Paavilainen, P. (2013). The mismatch-negativity (MMN) component of the auditory event-related potential to violations of abstract regularities: A review. *International Journal of Psychophysiology*, 88(2), 109–123. <https://doi.org/10.1016/j.ijpsycho.2013.03.015>
- Paavilainen, P., Arajärvi, P., & Takegata, R. (2007). Preattentive detection of nonsalient contingencies between auditory features. *Neuroreport*, 18(2), 159–163. <https://doi.org/10.1097/WNR.0b013e328010e2ac>
- Paavilainen, P., Valppu, S., & Näätänen, R. (2001). The additivity of the auditory feature analysis in the human brain as indexed by the mismatch negativity: 1+1 approximately 2 but 1+1+1<3. *Neuroscience Letters*, 301, 179–182. [https://doi.org/10.1016/S0304-3940\(01\)01635-4](https://doi.org/10.1016/S0304-3940(01)01635-4)
- Parks, N. A. (2013). Concurrent application of TMS and near-infrared optical imaging: Methodological considerations and potential artifacts. *Frontiers in Human Neuroscience*, 7(September), 592. <https://doi.org/10.3389/fnhum.2013.00592>
- Phillips, H. N., Blenkman, A., Hughes, L. E., Kochen, S., Bekinschtein, T. A., Cam, C. A. N., & Rowe, J. B. (2016). Convergent evidence for hierarchical prediction networks from human electrocorticography and magnetoencephalography. *Cortex*, 82, 192–205. <https://doi.org/10.1016/j.cortex.2016.05.001>
- Rinne, T., Alho, K., Ilmoniemi, R. J., Virtanen, J., & Näätänen, R. (2000). Separate time behaviors of the temporal and frontal mismatch negativity sources. *NeuroImage*, 12(1), 14–19. <https://doi.org/10.1006/nimg.2000.0591>
- Rinne, T., Degerman, A., & Alho, K. (2005). Superior temporal and inferior frontal cortices are activated by infrequent sound duration decrements: An fMRI study. *NeuroImage*, 26(1), 66–72. <https://doi.org/10.1016/j.neuroimage.2005.01.017>
- Rinne, T., Gratton, G., Fabiani, M., Cowan, N., Maclin, E., Stinard, A., ... Näätänen, R. (1999). Scalp-recorded optical signals make sound processing in the auditory cortex visible? *NeuroImage*, 10(5), 620–624. <https://doi.org/10.1006/nimg.1999.0495>
- Rossi, S., Hallett, M., Rossini, P. M., Pascual-Leone, A., Avanzini, G., Bestmann, S., ... Ziemann, U. (2009). Safety, ethical considerations, and application guidelines for the use of transcranial magnetic stimulation in clinical practice and research. *Clinical Neurophysiology*, 120(12), 2008–2039. <https://doi.org/10.1016/j.clinph.2009.08.016>
- Sable, J. J., Gratton, G., & Fabiani, M. (2003). Sound presentation rate is represented logarithmically in human cortex. *European Journal of Neuroscience*, 17(11), 2492–2496. <https://doi.org/10.1046/j.1460-9568.2003.02690.x>
- Sable, J. J., Low, K. A., Whalen, C. J., Maclin, E. L., Fabiani, M., & Gratton, G. (2007). Optical imaging of temporal integration in human auditory cortex. *European Journal of Neuroscience*, 25(1), 298–306. <https://doi.org/10.1111/j.1460-9568.2006.05255.x>
- Sams, M., Paavilainen, P., Alho, K., & Näätänen, R. (1985). Auditory frequency discrimination and event-related potentials. *Electroencephalography and Clinical Neurophysiology: Evoked Potentials*, 62(6), 437–448. [https://doi.org/10.1016/0168-5597\(85\)90054-1](https://doi.org/10.1016/0168-5597(85)90054-1)
- Sarrinen, J., Paavilainen, P., Schröger, E., Tervaniemi, M., & Näätänen, R. (1992). Representation of abstract attributes of auditory stimuli in the human brain. *Neuroreport*, 3, 1149–1151.
- Schall, U., Johnston, P., Todd, J., Ward, P. B., & Michie, P. T. (2003). Functional neuroanatomy of auditory mismatch processing: An event-related fMRI study of duration-deviant oddballs. *NeuroImage*, 20(2), 729–736. [https://doi.org/10.1016/S1053-8119\(03\)00398-7](https://doi.org/10.1016/S1053-8119(03)00398-7)
- Schröger, E., Bendixen, A., Trujillo-Barreto, N. J., & Roeber, U. (2007). Processing of abstract rule violations in audition. *PLoS One*, 2(11), e1131. <https://doi.org/10.1371/journal.pone.0001131>
- Sussman, E., Gomes, H., Nousak, J. M. K., Ritter, W., & Vaughan, H. G. (1998). Feature conjunctions and auditory sensory memory. *Brain Research*, 793(1–2), 95–102. [https://doi.org/10.1016/S0006-8993\(98\)00164-4](https://doi.org/10.1016/S0006-8993(98)00164-4)
- Suzuki, Y., & Takeshima, H. (2004). Equal-loudness-level contours for pure tones. *The Journal of the Acoustical Society of America*, 116(2), 918–933. <https://doi.org/10.1121/1.1763601>
- Szycik, G. R., Stadler, J., Brechmann, A., & Münte, T. F. (2013). Preattentive mechanisms of change detection in early auditory cortex: A 7 Tesla fMRI study. *Neuroscience*, 253, 100–109. <https://doi.org/10.1016/j.neuroscience.2013.08.039>
- Takegata, R., Huotilainen, M., Rinne, T., Näätänen, R., & Winkler, I. (2001). Changes in acoustic features and their conjunctions are processed by separate neuronal populations. *Neuroreport*, 12(3), 525–529. <https://doi.org/10.1097/00001756-200103050-00019>
- Talairach, J., & Tournoux, P. (1988). *Co-planar stereotaxic atlas of the human brain. 3-Dimensional proportional system: An approach to cerebral imaging*. New York, NY: Thieme Retrieved from citeulike-article-id: 745727.
- Tse, C.-Y., Gordon, B. A., Fabiani, M., & Gratton, G. (2010). Frequency analysis of the visual steady-state response measured with the fast optical signal in younger and older adults. *Biological Psychology*, 85(1), 79–89. <https://doi.org/10.1016/j.biopsycho.2010.05.007>
- Tse, C.-Y., Gratton, G., Garnsey, S. M., Novak, M. A., & Fabiani, M. (2015). Read my lips: Brain dynamics associated with audiovisual integration and deviance detection. *Journal of Cognitive Neuroscience*, 27(9), 1723–1737. <https://doi.org/10.1162/jocn>
- Tse, C.-Y., Low, K. A., Fabiani, M., & Gratton, G. (2012). Rules rule! Brain activity dissociates the representations of stimulus contingencies with

- varying levels of complexity. *Journal of Cognitive Neuroscience*, 24(9), 1941–1959. https://doi.org/10.1162/jocn_a_00229
- Tse, C.-Y., & Penney, T. B. (2007). Preattentive change detection using the event-related optical signal. *IEEE Engineering in Medicine and Biology Magazine*, 26(4), 52–58. <https://doi.org/10.1109/MEMB.2007.384096>
- Tse, C.-Y., & Penney, T. B. (2008). On the functional role of temporal and frontal cortex activation in passive detection of auditory deviance. *NeuroImage*, 41(4), 1462–1470. <https://doi.org/10.1016/j.neuroimage.2008.03.043>
- Tse, C.-Y., Rinne, T., Ng, K. K., & Penney, T. B. (2013). The functional role of the frontal cortex in pre-attentive auditory change detection. *NeuroImage*, 83, 870–879. <https://doi.org/10.1016/j.neuroimage.2013.07.037>
- Tse, C.-Y., Tien, K. R., & Penney, T. B. (2006). Event-related optical imaging reveals the temporal dynamics of right temporal and frontal cortex activation in pre-attentive change detection. *NeuroImage*, 29(1), 314–320. <https://doi.org/10.1016/j.neuroimage.2005.07.013>
- Tse, C.-Y., Yip, L., Lui, T. K., Xiao, X., Wang, Y., Chiu, W., ... Chan, S. S. (2018). Establishing the functional connectivity of the frontotemporal network in pre-attentive change detection with transcranial magnetic stimulation and event-related optical signal. *NeuroImage*, 179(March), 403–413. <https://doi.org/10.1016/j.neuroimage.2018.06.053>
- Wassermann, E. M., & Wassermann, E. M. (1998). Risk and safety of repetitive transcranial magnetic stimulation. *Electroencephalography and Clinical Neurophysiology*, 108, 1–16. [https://doi.org/10.1016/S0168-5597\(97\)00096-8](https://doi.org/10.1016/S0168-5597(97)00096-8)
- Whalen, C., Maclin, E. L., Fabiani, M., & Gratton, G. (2008). Validation of a method for coregistering scalp recording locations with 3D structural MR images. *Human Brain Mapping*, 29(11), 1288–1301. <https://doi.org/10.1002/hbm.20465>
- Winkler, I. (2007). Interpreting the mismatch negativity. *Journal of Psychophysiology*, 21(1992), 147–163. <https://doi.org/10.1027/0269-8803.21.3.147>
- Winkler, I., & Schröger, E. (2015). Auditory perceptual objects as generative models: Setting the stage for communication by sound. *Brain and Language*, 148, 1–22. <https://doi.org/10.1016/j.bandl.2015.05.003>
- Wolf, U., Wolf, M., Toronov, V., Gratton, E., Wolf, M., Wolf, U., ... Michalos, A. (2000). *Detecting cerebral functional slow and fast signals by frequency-domain near-infrared spectroscopy using two different sensors*. In T. Li (Ed.), *Biomedical Optical Spectroscopy and Diagnostics* (Vol. 38, TuF10). Miami, FL: Optical Society of America. <https://doi.org/10.1364/bosd.2000.tuf10>
- Wolff, C., & Schröger, E. (2001). Human pre-attentive auditory change-detection with single, double, and triple deviations as revealed by mismatch negativity additivity. *Neuroscience Letters*, 311(1), 37–40. [https://doi.org/10.1016/S0304-3940\(01\)02135-8](https://doi.org/10.1016/S0304-3940(01)02135-8)
- Xiao, X.-Z., Wong, H. K., Wang, Y., Zhao, K., Zeng, G. Q., Yip, L.-Y., ... Tse, C.-Y. (2018). Detecting violation in abstract pitch patterns with mismatch negativity. *Psychophysiology*, 55(8), e13078. <https://doi.org/10.1111/psyp.13078>

How to cite this article: Xiao X-Z, Shum Y-H, Lui TK-Y, et al. Functional connectivity of the frontotemporal network in preattentive detection of abstract changes: Perturbs and observes with transcranial magnetic stimulation and event-related optical signal. *Hum Brain Mapp*. 2020;41:2883–2897. <https://doi.org/10.1002/hbm.24984>